ЖУРНАЛ ФІЗИЧНИХ ДОСЛІДЖЕНЬ
т. 14, № 1 (2010) 1701(17 с.)

JOURNAL OF PHYSICAL STUDIES
v. 14, No. 1 (2010) 1701(17 p.)

LONGITUDINAL DIELECTRIC, PIEZOELECTRIC, ELASTIC, AND THERMAL CHARACTERISTICS OF THE KH_2PO_4 TYPE FERROELECTRICS

R. R. Levitskii[1], I. R. Zachek[2], A. S. Vdovych[1], A. P. Moina[1]
[1] *Institute for Condensed Matter Physics of the National Academy of Sciences of Ukraine 1, Svientsitskii St., 79011, Lviv, Ukraine*
[2] *Lviv Polytechnic National University 12, Bandery St., 79013, Lviv, Ukraine*
(Received January 1, 2009; received in final form January 4, 2010)

Within the framework of the modified proton ordering model for the KH_2PO_4 type with taking into account a linear in strain ε_6 contribution to the proton subsystem energy but without tunneling, in the four-particle cluster approximation we calculate the thermodynamic potentials of the system. Using the appropriate equations of state, we calculate spontaneous polarization, longitudinal dielectric permittivity of mechanically free and clamped crystals, their piezoelectric characteristics, elastic constants and molar specific heat. At the proper choice of the values of model parameters we obtain a good quantitative description of available experimental data for the $K(H_{1-x}D_x)_2PO_4$ type ferroelectrics.

Key words: ferroelectrics, cluster approximation, dielectric permittivity, piezoelectric modules.

PACS number(s): 77.80.−e, 77.84.−s, 77.84.Fa, 77.65.Bn

I. INTRODUCTION

Ferroelectrics of the MD_2XO_4 (M = K, Rb; X = P, As) in the paraelectric phase crystallize in the $\bar{4}\cdot m$ class of the tetragonal singony (space group $I\bar{4}2d$ with a non-center-symmetric point group D_{2d}^{12}). In the ferroelectric phase the space group of these compounds is Fdd (the point group C_{2v}^{19}) of the rhombic syngony with the axes rotated with respect to the crystallographic axes of the paraelectric phase by 45°. Thus, the MD_2XO_4 type crystals are non-centrosymmetric and possess piezoelectric properties in both phases which essentially affects their physical characteristics, particularly their dielectric response. Spontaneous polarization in these crystals is directed along the c axis and accompanied by spontaneous strain ε_6. So far, the theoretical description of the dielectric properties of the MD_2XO_4 type ferroelectrics within the conventional proton ordering model (see [1]) has been restricted by the static limit and the high-frequency relaxation. Attempts to explore the piezoelectric resonance phenomenon within the model that does not take into account the piezoelectric coupling were pointless. It should be also noted that qualitatively correct results for the MD_2XO_4 type compounds can be obtained only with taking into account the piezoelectric interactions. The conventional proton ordering model does not allow description of the effects related to the difference between the regimes of free and clamped crystals and is not able to reproduce the effect of crystal clamping by high-frequency electric fields.

In the presence of electric fields and shear stresses of certain symmetries the role of piezoelectric coupling in the phase transition and in the formation of the physical properties of the crystals can be explored.

Fundamental results for the KH_2PO_4 family ferroelectric have been obtained in [2–10]. For deformed crystals of the KH_2PO_4 type the Hamiltonian of the proton ordering model has been modified for the first time [2, 3] by taking into account the influence of the strain ε_6, deformational molecular field and splitting of lateral proton configurations only. Later [4, 5] all possible splittings of proton configurations induced by the strain ε_6 were taken into account. In [4] the phase transition, thermodynamic and longitudinal dielectric, piezoelectric, and elastic characteristics of the $K(H_{0.12}D_{0.88})_2PO_4$ crystal were calculated for the first time, and the influence of the σ_6 stress on these characteristics was explored. The same characteristics for the non-deuterated KH_2PO_4 crystals with taking into account tunneling and piezoelectric coupling were explored in [5, 6]. At the proper choice of the theory parameters a good quantitative description of experimental data for KH_2PO_4 is obtained. It should be noted that when tunneling is taken into account within a cluster approach, a non-physical behavior of the calculated characteristics appears at low temperature [11]. In [7–9] the influence of the electric field E_3 on the phase transition and physical characteristics of the $K(H_{0.12}D_{0.88})_2PO_4$ and KH_2PO_4 ferroelectrics was explored. A good agreement between the obtained results and the corresponding experimental data was obtained. It should be also mentioned that in [10] a mechanism of spontaneous strain ε_6 formation in the KH_2PO_4 type ferroelectrics and the role of proton coupling with acoustic lattice vibrations were explored in details.

In [4–8] the dynamic properties of the KH_2PO_4 family ferroelectrics were not considered. The investigation of these properties with taking into account the piezoelectric coupling is an important problem. Since the calculations of dynamical characteristics of these crystals within the cluster approximation with tunneling being taken into account are extremely difficult, and since tunneling has been found suppressed in these crystals by the short-range correlations [12], it is expedient to approach this problem by neglecting tunneling. In [13] within the

modified proton ordering model [4, 5] the thermal and longitudinal dielectric, piezoelectric, and elastic characteristics of the $K(H_{1-x}D_x)_2XO_4$ type ferroelectrics are calculated. Also, the relaxational phenomena in mechanically free and clamped crystals of this type are explored; ultrasound velocity and attenuation are calculated. It is shown that to determine the optimal values of the theory parameters, one has to take into account the experimental data for the longitudinal dynamic characteristics of the crystals. The effect of crystal clamping by high-frequency electric field, piezoelectric resonance and UHF dispersion, that is observed experimentally was discribed. Also, the peculiarities of sound attenuation near the phase transition points where considered.

In the present paper, within the framework of the modified proton ordering model for the KH_2PO_4 type with taking into account a linear in strain ε_6 contribution to the proton subsystem energy but without tunneling, in the four-particle cluster approximation we calculate thermodynamic and longitudinal piezoelectric, elastic, and dielectric characteristics of the $M(H_{1-x}D_x)_2XO_4$ type ferroelectrics. Using the obtained theoretical results an analysis of the available experimental data is performed.

II. CRYSTAL HAMILTONIAN

We shall consider a system of deuterons moving on the O–D...O bonds in deuterated ferroelectric MD_2XO_4 crystals. The reference system (x, y, z), also denoted as $(1, 2, 3)$, coincides with the tetragonal ($I\bar{4}2d$) crystallographic reference system (a,b,c). The primitive cell of the Bravais lattice of these crystals consists of two neighboring tetrahedra PO_4 along with four hydrogen bonds attached to one of them (the "A" type tetrahedron). The hydrogen bonds attached to the other tetrahedron ("B" type) belong to four surrounding it structural elements (Fig. 1).

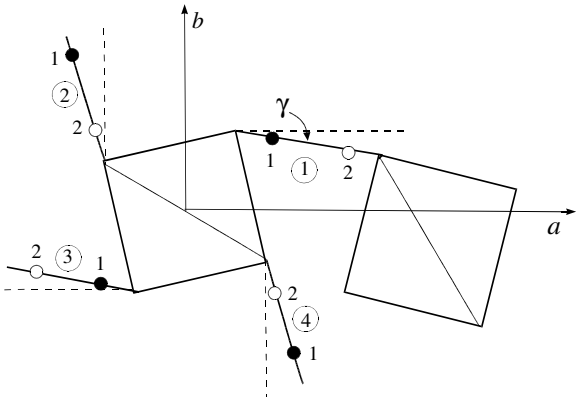

Fig. 1. A primitive cell of MD_2XO_4 crystals. One of possible ferroelectric proton configurations is shown.

The Hamiltonian of the deuteron subsystem with taking into account short-range and long-range interactions in the presence of external mechanical stress $\sigma_6 = \sigma_{xy}$ and electric field E_3 applied along the crystallographic axis **c**, inducing contributions to the strain ε_6 and polarization P_3 consists of the "seed" and pseudospin parts [4, 5]:

$$\hat{H} = NH^{(0)} + \hat{H}_s, \tag{2.1}$$

where N is the total number of primitive cells. The "seed" energy of a primitive cell corresponds to the heavy ions lattice and is explicitly independent of the hydrogen bonds configurations. It is expressed in terms of the strain ε_6 and the electric field E_3 and includes the elastic, piezoelectric, and dielectric parts

$$H^{(0)} = v\left(\frac{1}{2}c_{66}^{E0}\varepsilon_6^2 - e_{36}^0 E_3\varepsilon_6 - \frac{1}{2}\chi_{33}^{\varepsilon 0}E_3^2\right), \tag{2.2}$$

v is the primitive cell volume; c_{66}^{E0}, e_{36}^0, $\chi_{33}^{\varepsilon 0}$ are the "seed" elastic constant, coefficient of piezoelectric stress, and dielectric susceptibility, respectively. These quantities determine the temperature behavior of the corresponding characteristics of the studied crystals far from the transition temperature T_c.

The pseudospin part of the Hamiltonian reads

$$\hat{H}_s = \frac{1}{2}\sum_{\substack{qf\\ q'f'}} J_{ff'}(qq')\frac{\sigma_{qf}}{2}\frac{\sigma_{q'f'}}{2} + \hat{H}_{si}(6) + \sum_{qf} 2\psi_6\varepsilon_6\frac{\sigma_{qf}}{2} - \sum_{qf}\mu_{f3}E_3\frac{\sigma_{qf}}{2}. \tag{2.3}$$

Here the first term describes effective long-range interactions between deuterons including indirect lattice mediated interactions [14,15]; σ_{qf} is the z-th component of the pseudospin operator, describing the state of a deuteron in the q-th cell on the f-th bond ($f = 1, 2, 3, 4$). Two eigenvalues of the operator $\sigma_{qf} = \pm 1$ correspond to two possible positions of the deuteron on the bond (positions "1", "2" in Fig. 1).

In (2.3) $\hat{H}_{si}(6)$ is the linear over the strain ε_6 Hamiltonian of short-range interactions between deuterons near the PO_4 groups. In the absence of the strain ε_6 and field E_3 the short-range Hamiltonian of deuterons in the KD_2PO_4 crystal was obtained within the Slater–Takagi model [15, 16], where the energy of upper/lower deuteron configurations ε_s are twice degenerate, lateral configurations ε_a are four-fold degenerate, the single-ionized configurations ε_1 are eight-fold degenerate, and double-ionized configurations ε_0 are twice degenerate ($\varepsilon_s < \varepsilon_a \ll \varepsilon_1 \ll \varepsilon_0$).

In the presence of the strain ε_6 and in the electric field E_3 the system loses symmetry with respect to the mirror rotation by $\pi/4$ around the c axis, and splitting of upper/lower, lateral, and single-ionized configurations takes place (Table 1). Since the strain ε_6 and polarization P_3 are transformed via the same irreducible representation (B_2 in the paraelectric phase and A_1 in the ferroelectric phase), the electric field E_3 does not split those levels, which remain degenerate in the presence of the strain ε_6 [17].

The Hamiltonian of the short-range interactions between deuterons

$$\hat{H}_{si}(6) = \sum_q [\hat{H}_6^A(q) + \hat{H}_6^B(q)],$$

describes the total configurational energy of crystal deuterons. Here $\hat{H}_6^{A,B}(q)$ are the Hamiltonians of the short-range configurations interactions of deuterons near PO_4 tetrahedra of the "A" and "B" types. Also

$$\hat{H}_6^A(q) = \sum_{i=1}^{16} \hat{N}_i^A(q) E_i(6),$$

where $\hat{N}_i(q) = \prod_{f=1}^{4} \frac{1}{2}(1 + s_f \frac{\hat{\sigma}_{qf}}{2})$ is the operator of the four-particle configuration [15, 16], where s_f is the sign of the eigenvalue of the $\hat{\sigma}_{qf}$ operator in a particular deuteron configuration "$s_1 s_2 s_3 s_4$": s_f="+" or "−"; $E_i(6)$ are the deuteron configuration energies (Table 1). The contributions of the two tetrahedra to the configurational energy of the primitive cell are the same [15].

i		E_{i6}	i		E_{i6}
1	++++	$\varepsilon_s - \delta_{s6}\varepsilon_6 - \mu_3 E_3$	9	−−−+	$\varepsilon_1 - \delta_{16}\varepsilon_6 - \frac{\mu_3 E_3}{2}$
2	−−−−	$\varepsilon_s + \delta_{s6}\varepsilon_6 + \mu_3 E_3$	10	−−+−	
3	+−+−	ε_0	11	−+−−	
4	−+−+	ε_0	12	+−−−	
5	++−−	$\varepsilon_a + \delta_{a6}\varepsilon_6$	13	++−+	$\varepsilon_1 + \delta_{16}\varepsilon_6 + \frac{\mu_3 E_3}{2}$
6	−−++	$\varepsilon_a + \delta_{a6}\varepsilon_6$	14	+++−	
7	−++−	$\varepsilon_a - \delta_{a6}\varepsilon_6$	15	−+++	
8	+−−+	$\varepsilon_a - \delta_{a6}\varepsilon_6$	16	+−++	

Table 1. Energies of deuteron configurations near the PO_4 groups.

Finally, the Hamiltonian $\hat{H}_{si}(6)$ takes the form

$$\begin{aligned}\hat{H}_{si}(6) = \sum_q \Bigg\{ & \left(\frac{\delta_{s6}}{8}\varepsilon_6 + \frac{\delta_{16}}{4}\varepsilon_6\right)(\sigma_{q1} + \sigma_{q2} + \sigma_{q3} + \sigma_{q4}) \\ & + \left(\frac{\delta_{s6}}{8}\varepsilon_6 - \frac{\delta_{16}}{4}\varepsilon_6\right)(\sigma_{q1}\sigma_{q2}\sigma_{q3} + \sigma_{q1}\sigma_{q2}\sigma_{q4} + \sigma_{q1}\sigma_{q3}\sigma_{q4} + \sigma_{q2}\sigma_{q3}\sigma_{q4}) \\ & + \frac{1}{4}(V + \delta_{a6}\varepsilon_6)(\sigma_{q1}\sigma_{q2} + \sigma_{q3}\sigma_{q4}) + \frac{1}{4}(V - \delta_{a6}\varepsilon_6)(\sigma_{q2}\sigma_{q3} + \sigma_{q4}\sigma_{q1}) \\ & + \frac{1}{4}U(\sigma_{q1}\sigma_{q3} + \sigma_{q2}\sigma_{q4}) + \frac{1}{16}\Phi\sigma_{q1}\sigma_{q2}\sigma_{q3}\sigma_{q4},\end{aligned} \tag{2.4}$$

Here

$$V = -\frac{1}{2}w_1, \qquad U = \frac{1}{2}w_1 - \varepsilon, \qquad \Phi = 4\varepsilon - 8w + 2w_1,$$

and

$$\varepsilon = \varepsilon_a - \varepsilon_s, \qquad w = \varepsilon_1 - \varepsilon_s, \qquad w_1 = \varepsilon_0 - \varepsilon_s,$$

where ε_s, ε_a, ε_1, ε_0 are the deuteron configuration energies, and ε w, w_1 are the ferroelectric energies of the extended Slater–Takagi model [15, 16].

The third term in (2.3) is the linear over the shear strain ε_6 mean field Hamiltonian, induced by the piezoelectric coupling; ψ_6 — is the parameter of the deformational molecular field.

The last term in (2.3) effectively describes interactions of deuterons with the external electric field E_3. Here μ_{f3} is the effective dipole moment of the f-th hydrogen bond, and

$$\mu_{13} = \mu_{23} = \mu_{33} = \mu_{43} = \mu_3 = \frac{1}{2}\mu_{3s} + \mu_3^{(d)},$$

where μ_{3s} is the dipole moment of upper/lower configurations, and $\mu_3^{(d)}$ is the projections of the dipole moment of a deuteron bond [17].

Considering the peculiarities of the crystal structure of the $M\mathrm{D}_2X\mathrm{O}_4$ type ferroelectrics, the thermodynamic potential of the system will be calculated using the four-particle cluster approximation for the short-range interactions [15,16]. The long-range interactions are taken into account in the mean field approximation. In the cluster approach the thermodynamic potential of the $M\mathrm{D}_2X\mathrm{O}_4$ per primitive cell reads

$$g(6) = H^{(0)} + 2\nu_c[\eta^{(1)}(6)]^2 + \frac{1}{2}T\sum_{f=1}^{4}\ln Z_{1f} - T\ln Z_4 - \bar{v}\sigma_6\varepsilon_6, \qquad \bar{v} = \frac{v}{k_{\mathrm{B}}}, \tag{2.5}$$

where $4\nu_c = J_{11}(0) + 2J_{12}(0) + J_{13}(0)$ is the eigenvalue of the Fourier transform of the long-range interaction matrix $J_{ff'} = \sum\limits_{\mathbf{R}_q - \mathbf{R}_{q'}} J_{ff'}(qq')$;

$$\eta^{(1)}(6) = \langle\sigma_{q1}\rangle = \langle\sigma_{q2}\rangle = \langle\sigma_{q3}\rangle = \langle\sigma_{q4}\rangle$$

is the parameter of deuteron ordering; $Z_{1f} = \mathrm{Sp}\, e^{-\beta\hat{H}_{qf}^{(1)}}$, $Z_4 = \mathrm{Sp}\, e^{-\beta\hat{H}_{q6}^{(4)}}$ $\beta = \frac{1}{k_{\mathrm{B}}T}$ are the single-particle and four-particle partition functions. The single-particle $\hat{H}_{qf}^{(1)}$ and four-particle $\hat{H}_{q6}^{(4)}$ deuteron Hamiltonians are

$$\hat{H}_{qf}^{(1)} = -\frac{\bar{z}_{f6}}{\beta}\frac{\sigma_{qf}}{2}, \tag{2.6}$$

$$\begin{aligned}\hat{H}_{q6}^{(4)} = &-\sum_{f=1}^{4}\frac{z_6}{\beta}\frac{\sigma_{qf}}{2} + \frac{\varepsilon_6}{4}(-\delta_{s6} + 2\delta_{16})\sum_{f=1}^{4}\frac{\sigma_{qf}}{2} \\ &- \varepsilon_6(\delta_{s6}+2\delta_{16})\left(\frac{\sigma_{q1}}{2}\frac{\sigma_{q2}}{2}\frac{\sigma_{q3}}{2} + \frac{\sigma_{q1}}{2}\frac{\sigma_{q2}}{2}\frac{\sigma_{q4}}{2} + \frac{\sigma_{q1}}{2}\frac{\sigma_{q3}}{2}\frac{\sigma_{q4}}{2} + \frac{\sigma_{q2}}{2}\frac{\sigma_{q3}}{2}\frac{\sigma_{q4}}{2}\right) \\ &+ (V + \delta_{a6}\varepsilon_6)\left(\frac{\sigma_{q1}}{2}\frac{\sigma_{q2}}{2} + \frac{\sigma_{q3}}{2}\frac{\sigma_{q4}}{2}\right) + (V - \delta_{a6}\varepsilon_6)\left(\frac{\sigma_{q2}}{2}\frac{\sigma_{q3}}{2} + \frac{\sigma_{q4}}{2}\frac{\sigma_{q1}}{2}\right) \\ &+ U\left(\frac{\sigma_{q1}}{2}\frac{\sigma_{q3}}{2} + \frac{\sigma_{q2}}{2}\frac{\sigma_{q4}}{2}\right) + \Phi\frac{\sigma_{q1}}{2}\frac{\sigma_{q2}}{2}\frac{\sigma_{q3}}{2}\frac{\sigma_{q4}}{2},\end{aligned} \tag{2.7}$$

where

$$z_6 = \beta(-\Delta^c + 2\nu_c\eta^{(1)}(6) - 2\psi_6\varepsilon_6 + \mu_3 E_3),$$

$$\bar{z}_{f6} = \beta[-2\Delta^c + 2\nu_c\eta^{(1)}(6) - 2\psi_6\varepsilon_6 + \mu_3 E_3].$$

The effective field Δ^c created by the neighboring bonds from outside the cluster can be determined from the self-consistency condition, which states that the mean values of pseudospins $\langle\sigma_{qf}\rangle$ calculated within the four-particle and one-particle cluster approximations should coincide, that is,

$$\langle\sigma_{qf}\rangle = \frac{\mathrm{Sp}\left\{\sigma_{qf}e^{-\beta\hat{H}_{q6}^{(4)}}\right\}}{\mathrm{Sp}\, e^{-\beta\hat{H}_{q6}^{(4)}}} = \frac{\mathrm{Sp}\left\{\sigma_{qf}e^{-\beta\hat{H}_{qf}^{(1)}}\right\}}{\mathrm{Sp}\, e^{-\beta\hat{H}_{qf}^{(1)}}}. \tag{2.8}$$

The field Δ^c are determined from the condition of the thermodynamic potential minimum (2.5):

$$\frac{\partial g}{\partial\Delta^c} = 0.$$

Finally, the single-particle deuteron distribution functions can be obtained in the following form

$$\eta^{(1)}(6) = \frac{m_6}{D_6}, \tag{2.9}$$

where

$$m_6 = \sinh(2z_6 + \beta\delta_{s6}\varepsilon_6) + 2b\sinh(z_6 - \beta\delta_{16}\varepsilon_6),$$

$$D_6 = \cosh(2z_6 + \beta\delta_{s6}\varepsilon_6) + 4b\cosh(z_6 - \beta\delta_{16}\varepsilon_6) + 2a\cosh\beta\delta_{a6}\varepsilon_6 + d,$$

$$z_6 = \frac{1}{2}\ln\frac{1+\eta^{(1)}(6)}{1-\eta^{(1)}(6)} + \beta\nu_c\eta^{(1)}(6) - \beta\psi_6\varepsilon_6 + \frac{\beta\mu_3}{2}E_3,$$

$$a = e^{-\beta\varepsilon}, \qquad b = e^{-\beta w}, \qquad d = e^{-\beta w_1}.$$

Calculating the eigenvalues of the cluster and single-particle Hamiltonians, we obtain the single-particle and four-particle partition functions and write the thermodynamic potentical (2.5) as

$$g(6) = \frac{\bar v}{2} c_{66}^{E0} \varepsilon_6^2 - \bar v e_{36}^0 \varepsilon_6 E_3 - \frac{\bar v}{2} \chi_{33}^{\varepsilon 0} E_3^2 + 2T \ln 2 \qquad (2.10)$$
$$+2\bar\nu_c [\eta^{(1)}(6)]^2 - 2T \ln[1 - (\eta^{(1)}(6))^2] - 2T \ln D_6 - \bar v \sigma_6 \varepsilon_6.$$

Now we shall calculate the dielectric, piezoelectric, elastic, and thermal characteristics of $M\mathrm{D}_2X\mathrm{O}_4$ ferroelectrics.

Using the dielectric, elastic, and thermal equations of state

$$P_3 = -\frac{1}{\bar v}\left(\frac{\partial g(6)}{\partial E_3}\right)_{T,\sigma_6}, \qquad \frac{1}{\bar v}\left(\frac{\partial g(6)}{\partial \varepsilon_6}\right)_{T,E_3,\sigma_6} = 0,$$
$$S_6 = -R\left(\frac{\partial g(6)}{\partial T}\right)_{E_3,\sigma_6}$$

and the thermodynamic potential (2.10) we obtain expressions for polarization P_3, stress σ_6 (an equation for the strain ε_6) and molar entropy of the deuteron subsystem (here R is the gas constant)

$$P_3 = e_{36}^0 \varepsilon_6 + \chi_{33}^{\varepsilon 0} E_3 + 2\frac{\mu}{v}\frac{m(6)}{D_6}, \qquad (2.11)$$

$$\sigma_6 = c_{66}^{E0}\varepsilon_6 - e_{36}^0 E_3 + \frac{4\psi_6}{v}\frac{m(6)}{D_6} + \frac{2\delta_{a6}}{\bar v D_6^z} M_{a6}$$
$$- \frac{2\delta_{s6}}{vD_6} M_{s6} + \frac{2\delta_{16}}{vD_6} M_{16}, \qquad (2.12)$$

$$S_6 = R\Big\{2\ln 2 + 2\ln[1 - (\eta^{(1)}(6))^2] + 2\ln D_6$$
$$+ 4T\varphi_6^T \eta^{(1)}(6) + \frac{2M_6}{D_6}\Big\}. \qquad (2.13)$$

Here we use the following notations

$$M_{a6} = 2a\sinh\beta\delta_{a6}\varepsilon_6, \qquad M_{s6} = \sinh(2z_6 + \beta\delta_{s6}\varepsilon_6),$$
$$M_{16} = 4b\sinh(z_6 - \beta\delta_{16}\varepsilon_6),$$
$$\varphi_6^T = -\frac{1}{T^2}(\nu_c\eta^{(1)}(6) - \psi_6\varepsilon_6),$$
$$M_6 = \beta w 4b\cosh(z_6 - \beta\delta_{16}\varepsilon_6) + \beta w_1 d$$
$$+ \beta\varepsilon 2a\cosh\beta\delta_{a6}\varepsilon_6 + \beta\varepsilon_6 r_6,$$
$$r_6 = -\delta_{s6}M_{s6} - \delta_{a6}M_{a6} + \delta_{16}M_{16}.$$

From Eq. (2.11), (2.12) we find the isothermic dielectric susceptibility of a clamped crystal ($\varepsilon_6 = \mathrm{const}$):

$$\chi_{33}^{T\varepsilon} = \left(\frac{\partial P_3}{\partial E_3}\right)_{T,\varepsilon_6} = \chi_{33}^0 + \bar v\frac{\mu^2}{v^2}\frac{1}{T}\frac{2\varkappa_6}{D_6 - 2\varkappa_6\varphi_6^\eta}, \quad (2.14)$$

where

$$\varkappa_6 = \cosh(2z_6 + \beta\delta_{s6}\varepsilon_6) + b\cosh(z_6 - \beta\delta_{16}\varepsilon_6)$$
$$- \eta^{(1)}(6)m_6,$$
$$\varphi_6^\eta = \frac{1}{1 - (\eta^{(1)}(6))^2} + \beta\nu_c;$$

isothermic coefficient of piezoelectric stress e_{36}^T

$$e_{36}^T = -\left(\frac{\partial\sigma_6}{\partial E_3}\right)_{T,\varepsilon_6} = \left(\frac{\partial P_3}{\partial\varepsilon_6}\right)_{T,E_3}$$
$$= e_{36}^0 + \frac{2\mu_3}{v}\frac{\beta\theta_6}{D_6 - 2\varphi_6^\eta\varkappa_6}. \qquad (2.15)$$

where

$$\theta_6 = -2\varkappa_6^c\psi_6 + f_6,$$
$$f_6 = \delta_{s6}\cosh(2z_6 + \beta\delta_{s6}\varepsilon_6) - 2b\delta_{16}\cosh(z_6 - \beta\delta_{16}\varepsilon_6)$$
$$+ \eta^{(1)z}(6)(-\delta_{s6}M_{s6} + \delta_{a6}M_{a6} + \delta_{16}M_{16});$$

isothermic elastic constant at constant field

$$c_{66}^{TE} = c_{66}^{E0} + \frac{8\psi_6}{v}\cdot\frac{\beta(-\psi_6\varkappa_6^c + f_6)}{D_6 - 2\varphi_6^\eta\varkappa_6}$$
$$- \frac{4\beta\varphi_6^\eta f_6^2}{vD_6(D_6 - 2\varphi_6^\eta\varkappa_6)} - \frac{2\beta}{vD_6}[\delta_{s6}^2\cosh(2z_6 + \beta\delta_{s6}\varepsilon_6)$$
$$+ \delta_{a6}^2 2a\cosh\beta\delta_{a6}\varepsilon_6 + \delta_{16}^2 4b\cosh(z_6 - \beta\delta_{16}\varepsilon_6)]$$
$$+ \frac{2\beta}{vD_6^2}(-\delta_{s6}M_{s6} + \delta_{a6}M_{a6} + \delta_{16}M_{16})^2. \qquad (2.16)$$

In the paraelectric phase and in the absence of external fields, that is at $E_3 = 0$, $\sigma_6 = 0$, the above-calculated characteristics have much simpler form

$$\chi_{33}^{T\varepsilon} = \chi_{33}^{\varepsilon 0} + \bar v\frac{\mu_3^2}{v^2}\frac{\beta 2(1+b)}{-1 + 2b + 2a + d - 2\beta\nu_c(1+b)},$$
$$e_{36}^T = e_{36}^0 + \frac{\mu_3}{v}\frac{2\beta[-2(1+b)\psi_6 + \delta_{s6} - 2b\delta_{16}]}{-1 + 2b + 2a + d - 2\beta\nu_c(1+b)},$$
$$c_{66}^{TE} = c_{66}^{E0} + \frac{8\psi_6}{v}\frac{\beta[-2(1+b)\psi_6 + \delta_{s6} - 2b\delta_{16}]}{-1 + 2b + 2a + d - 2\beta\nu_c(1+b)}$$
$$- \frac{4\beta(1+\beta\nu_c)(\delta_{s6} - 2b\delta_{16})^2}{(1 + 4b + 2a + d)[-1 + 2b + 2a + d - 2\beta\nu_c(1+b)]}$$
$$+ \frac{2\beta}{v}\frac{\delta_{s6}^2 + 2a\delta_{a6}^2 + 4b\delta_{16}^2}{1 + 4b + 2a + d}.$$

The other isothermic dielectric, piezoelectric, and elastic characteristics can be expressed via the quantities found above using the known relations. Thus, the isothermic dielectlric susceptibility of a free crystal reads (σ_6=const)

$$\chi_{33}^{T\sigma} = \left(\frac{\partial P_3}{\partial E_3}\right)_{T,\sigma_6} = \chi_{33}^{T\varepsilon} + \frac{(e_{36}^T)^2}{c_{66}^{TE}}$$
$$= \chi_{33}^{T\varepsilon} + e_{36}^T d_{36}^T; \qquad (2.17)$$

the isothermic coefficient of piezoelectric strain is

$$d_{36}^T = \left(\frac{\partial\varepsilon_6}{\partial E_3}\right)_{T,\sigma_6} = \left(\frac{\partial P_3}{\partial\sigma_6}\right)_{T,E_3} = \frac{e_{36}^T}{c_{66}^{TE}}, \qquad (2.18)$$

the isothermic constant of piezoelectric stress is

$$h_{36}^T = -\left(\frac{\partial E_3}{\partial \varepsilon_6}\right)_{T,P_3} = -\left(\frac{\partial \sigma_6}{\partial P_3}\right)_{T,\varepsilon_6} = \frac{e_{36}^T}{\chi_{33}^{T\varepsilon}}, \quad (2.19)$$

the isothermic constant of piezoelectric strain is

$$g_{36}^T = -\left(\frac{\partial E_3}{\partial \sigma_6}\right)_{T,P_3} = \left(\frac{\partial \varepsilon_6}{\partial P_3}\right)_{T,\sigma_6} = \frac{e_{36}^T}{\chi_{33}^{T\varepsilon} c_{66}^{TE} + (e_{36}^T)^2} = \frac{h_{36}^T}{c_{66}^{TP}}, \quad (2.20)$$

the isothemic elastic constant and the constant polarization is

$$c_{66}^{TP} = \left(\frac{\partial \sigma_6}{\partial \varepsilon_6}\right)_{T,P_3} = c_{66}^{TE} + e_{36}^T h_{36}^T = c_{66}^{TE} + \frac{(e_{36}^T)^2}{\chi_{33}^{T\varepsilon}}, \quad (2.21)$$

the isothermic compliances at constant field are

$$s_{66}^{TE} = \left(\frac{\partial \varepsilon_6}{\partial \sigma_6}\right)_{T,E_3} = \frac{1}{c_{66}^{TE}},$$
$$s_{66}^{TP} = \left(\frac{\partial \varepsilon_6}{\partial \sigma_6}\right)_{T,P_3} = \frac{1}{c_{66}^{TP}}. \quad (2.22)$$

The molar heat capacity of the deuteron subsystem of $M\mathrm{D_2}X\mathrm{O_4}$ crystals can be found from the entropy (2.13)

$$\Delta C_6^\sigma = T\left(\frac{\partial S}{\partial T}\right)_\sigma = \Delta C_6^\varepsilon + q_6^P \alpha_6, \quad (2.23)$$

where ΔC_6^ε is the molar specific heat at constant strain

$$\Delta C_6^\varepsilon = q_6^{P,\varepsilon} + q_6^\varepsilon p_6^\sigma. \quad (2.24)$$

Using (2.13), we easily obtain

$$q_6^{P,\varepsilon} = \left(\frac{\partial S_6}{\partial T}\right)_{P_3,\varepsilon_6} = \frac{2R}{D_6}\left\{2T\varphi_6^T(q_6 - \eta^{(1)}(6)M_6) + N_6 - \frac{M_6^2}{D_6}\right\}, \quad (2.25)$$
$$q_6^\varepsilon = \left(\frac{\partial S_6}{\partial P_3}\right)_{\varepsilon_6,T} = \frac{v}{\mu_3}\frac{2RT}{D_6}\{D_6 T\varphi_6^T + [q_6 - \eta^{(1)}(6)M_6]\varphi_6^\eta\}$$

is the heat of polarization at the given ε_6,

$$q_6^P = \left(\frac{\partial S_6}{\partial \varepsilon_6}\right)_{P_3,T} = \frac{2R}{D_6}\left\{2T\varphi_6^T(-2\varkappa_6\psi_6 + f_6) - 2[q_6 - \eta^{(1)}(6)M_6]\psi_6 - \lambda_6 + \frac{M_6}{D_6}r_6\right\},$$

is the heat of strain at the given P_3.

Here we used the following notations

$$N_6 = (\beta\varepsilon)^2 2a\cosh\beta\delta_{a6}\varepsilon_6 + (\beta w)^2 4b\cosh(z_6 - \beta\delta_{16}\varepsilon_6) + (\beta w_1)^2 d + \varepsilon_6(2\beta^2\varepsilon\delta_{a6}M_{a6} + 2\beta^2 w\delta_{16}M_{16}) + \varepsilon_6^2[(\beta\delta_{a6})^2 2a\cosh\beta\delta_{a6}\varepsilon_6 - (\beta\delta_{s6})^2\cosh(2z_6 + \beta\delta_{s6}\varepsilon_6) + (\beta\delta_{16})^2 4b\cosh(z_6 - \beta\delta_{16}\varepsilon_6)],$$

$$q_6 = \beta w 2b\cosh(z_6 - \beta\delta_{16}\varepsilon_6) + \varepsilon_6[-\beta\delta_{s6}\cosh(2z_6 + \beta\delta_{s6}\varepsilon_6) + \beta\delta_{16}\cosh(z_6 - \beta\delta_{16}\varepsilon_6)],$$

$$\lambda_6 = -\beta\varepsilon\delta_{a6}M_{a6} + \beta w\delta_{16}M_{16} + \varepsilon_6[-\beta\delta_{s6}^2\cosh(2z_6 + \beta\delta_{s6}\varepsilon_6) + \beta\delta_{a6}^2 2a\cosh\beta\delta_{a6}\varepsilon_6 + \beta\delta_{16}^2 4b\cosh(z_6 - \beta\delta_{16}\varepsilon_6)].$$

In (2.19) and (2.20) $p_6^\sigma = (\partial P_3/\partial T)_{\sigma,E_3}$ is the pyroelectric coefficient, and $\alpha_6 = (\partial\varepsilon_6/\partial T)_\sigma$ is the thermal expansion coefficient.

From (2.11) we get

$$p_6^\sigma = p_6^\varepsilon + e_{36}\alpha_6, \quad (2.26)$$

where

$$p_6^\varepsilon = \frac{\mu_3}{v}\frac{2}{T}\frac{2\varkappa_6 T\varphi_6^T + [q_6 - \eta^{(1)}(6)M_6]}{D_6 - 2\varkappa_6\varphi_6^\eta}, \quad (2.27)$$

and the thermal expansion coefficient is

$$\alpha_6 = \frac{-p_6 + h_{36}p_6^\varepsilon}{c_{66}^E}, \quad p_6 = \left(\frac{\partial \sigma_6}{\partial T}\right)_{p_3,\varepsilon_6} = q_6^p. \quad (2.28)$$

III. COMPARISON OF THE CALCULATED PHYSICAL CHARACTERISTICS OF THE KH_2PO_4 FAMILY CRYSTALS WITH EXPERIMENTAL DATA. DISCUSSION

Let us calculate thermal, piezoelectric, elastic, and longitudinal dielectric characteristics of the $M(\mathrm{H}_{1-x}\mathrm{D}_x)_2X\mathrm{O}_4$ type ferroelectrics obtained within

the developed theory numerically and compare the obtained results with the corresponding experimental data. It should be noted that the theory developed in previous sections is valid, strictly speaking, for completely deuterated crystals only. However, we shall consider also pure and partially deuterated crystals $x(0 \leqslant x \leqslant 1)$. The experimentally established relaxational character of the dielectric dispersion of $\varepsilon^*_{33}(\nu, T)$ and $\varepsilon^*_{11}(\nu, T)$ [18–22] in these crystals, according to [12, 23, 24], is most likely associated with the suppression of tunneling by the short-range interactions. Therefore, the tunneling effects in the considered crystals will be neglected. We shall assume that the proposed theory with the averaged effective parameters is valid for the $M(H_{1-x}D_x)_2XO_4$ crystals too.

To set the optimal values of the model parameters we have to use the dependence of the transition temperature T_c on the deuteron concentration x. We shall briefly analyze the experimental data for the $T_c(x)$ dependence in $M(H_{1-x}D_x)_2XO_4$ shown in Figs. 2,3.

In Fig. 2 a rather large dispersion of experimental points for $T_c(x)$ in $K(H_{1-x}D_x)_2PO_4$ obtained by different authors is seen.

In some papers [19,44,45] the dependence of the phase transition temperature in the $K(H_{1-x}D_x)_2PO_4$ crystals on x is considered to be linear and described by the empirical relation $T_c = 123{+}106x{\pm}2$ [19], $T_c = 121.7{+}107x$ [45]. In these papers usually too few concentrations are taken into account, and T_c is measured with insufficient precision. The measurements [35, 38, 46] free from these drawbacks yield non-linear dependences $T_c(x)$, however, with different dT_c/dx and the extrapolated values $T_c(1, 0)$. A thorough investigation [33,34] of the deuteration dependence of the phase transition temperature for a large number of samples of $K(H_{1-x}D_x)_2PO_4$ has confirmed the non-linear character of $T_c(x)$. Comparing the data of [33,34] with other measurements of $T_c(x)$ we can note that the values of $T_c(x)$ [33,34] agree with the data of [35,45] at $0 \leq x \leq 0.4$ and of [46] at $0 \leq x \leq 0.3$. Some values of T_c given in [19] at $x = 0.35; 0.68$ and in [45] at $x = 0.4$ coincide with the values of [33,34]. Overall, however, the values of $T_c(x)$ obtained in [19, 44–46] are by 5–10 K higher than those of [33, 34].

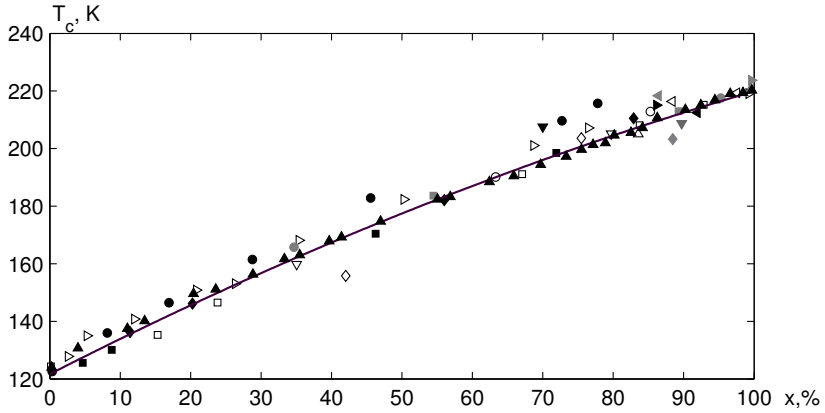

Fig. 2. Dependence of the phase transition temperature in $K(H_{1-x}D_x)_2PO_4$ on deuteron concentration x ○ [25], ● [26], ● [27], □ [18], ■ [28], ■ [29], ◇ [19], ◆ [30], ◆ [31], △ [32], ▲ [40], ▲ [33, 34], ▽ [35], ▼ [36], ▼ [37], ▷ [38], ▶ [39], ▶ [20], ◁ [41], ◀ [42], ◀ [43]. Line is the theoretical dependence $T_c(x)$.

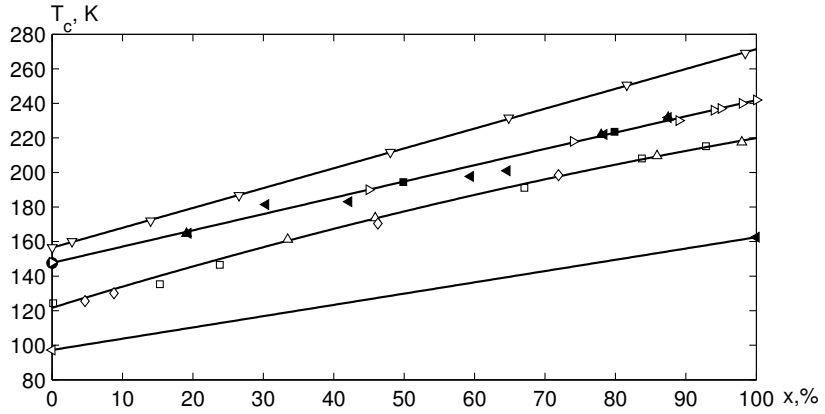

Fig. 3. Dependence of the phase transition temperature on deuteron concentration x in $Cs(H_{1-x}D_x)_2PO_4$ — ▽ [48], $Rb(H_{1-x}D_x)_2PO_4$ — ◀ [49], ■ [50], $K(H_{1-x}D_x)_2PO_4$ — ◇ [29], □ [18], △ [33,34], $K(H_{1-x}D_x)_2AsO_4$ — ◁ [51], ◀ [52], $N(H_{1-x}D_x)_4(H_{1-x}D_x)_2PO_4$ — ◀ [43]. Line is the theoretical dependence $T_c(x)$.

A rather large spread of the data is caused, most likely, by imprecise determination of the deuterium concentration in the samples of $K(H_{1-x}D_x)_2PO_4$. Hereafter, we shall use the values of $T_c(x)$ given in [33, 34]. Using this dependence $T_c(x)$ we can determine the correct values of deuteration in the samples of $K(H_{1-x}D_x)_2PO_4$. The solid line in Fig. 2 is the theoretical results for $T_c(x)$ obtained with the proposed theory.

In [47] an empirical dependence of the phase transition temperatures T_c in $Rb(H_{1-x}D_x)_2PO_4$ on deuterium concentration x was proposed, namely $T_c(x) = (146.6 + 108.0x)$K.

For the sake of comparison, in figure 3 we show the deuteration dependences of the transition temperatures in $Cs(H_{1-x}D_x)_2PO_4$, $M(H_{1-x}D_x)_2XO_4$, $N(H_{1-x}D_x)_4(H_{1-x}D_x)_2PO_4$. It turns out that the coefficient $\frac{dT_c(x)}{dx}$ is practically the same for all these crystals, whereas the dependences $T_c(x)$ for $Rb(H_{1-x}D_x)_2PO_4$ and $N(H_{1-x}D_x)_4(H_{1-x}D_x)_2PO_4$ coincide.

In order to evaluate the corresponding temperature and frequency dependences of the physical characteristics of the $M(H_{1-x}D_x)_2XO_4$ crystals using the expressions obtained in the previous sections, we have to set the values of the following parameters:

- energies of proton and deuteron configurations ε_H, w_H, w_{1H} and ε_D, w_D, w_{1D}, respectively;
- parameters of the long-range interactions $\nu_c(x)$;
- effective dipole moments μ_{3H}, μ_{3D};
- deformational potentials ψ_{6H}, $\psi_{6,012H}$, δ_{s6H}, $\delta_{s6,012H}$, δ_{a6H}, $\delta_{a6,012H}$, δ_{16H}, $\delta_{16,012H}$;
- "seed" dielectric susceptibilities $\chi^{\varepsilon 0}_{33H}$, $\chi^{\varepsilon 0}_{33D}$;
- "seed" elastic constants c^{E0}_{66H}, $c^{E0}_{66,012H}$;
- "seed" coefficients of piezoelectric stress e^0_{36H}, $e^0_{36,012H}$.

Here the subscript H denotes the parameters of MH_2XO_4 crystals, and the subscript D denotes the parameters for deuterated MD_2XO_4 crystals. We shall also assume that to the partially deuterated crystals $M(H_{1-x}D_x)_2PO_4$ the following averaged parameters correspond

$$\varepsilon(x) = \varepsilon_H(1-x) + \varepsilon_D x, \quad w(x) = w_H(1-x) + w_D x.$$

In addition to the mentioned parameters, to calculate the obtained physical characteristics of the $M(H_{1-x}D_x)_2XO_4$ crystals we have to set the volume of their primitive cells, consisting of two PO_4 groups. Since for $K(H_{1-x}D_x)_2PO_4$ $v(x) = [0,19359 + 0,00184x] \cdot 10^{-21}$ cm^3 [47], we use the following values of $v \cdot 10^{21}$ (cm^3): KH_2PO_4: 0.1936, KD_2PO_4: 0.1954, RbH_2PO_4: 0.2090, KH_2AsO_4: 0.2052, KD_2AsO_4: 0.2065.

The energy w_{1H} of two proton configurations with four or zero protons near the given oxygen tetrahedron should be much higher than ε_H and w_H. Therefore we take $w_{1H} = \infty$ and $w_{1D} = \infty$ ($d = 0$).

In order to determine the optimal values of the mentioned above parameters for the $M(H_{1-x}D_x)_2XO_4$ crystals we shall use the experimental data for their physical characteristics. For $K(H_{1-x}D_x)_2PO_4$: $T_c(x)$ [33, 34], $P_s(T)$ [35, 54], ε_6 [55, 56], $\Delta C_p(T)$ [57–59], $\varepsilon^\sigma_{33}(0,T)$ [55, 56] [35, 40, 51, 60], d_{36} [60–63], c^E_{66} [60, 64–66], $\varepsilon^{*\varepsilon}_{33}(\omega,T)$ [18]; for $Rb(H_{1-x}D_x)_2PO_4$: $T_c(x)$ [49], $P_s(T)$ [37], $\Delta C_p(T)$ [57], $\varepsilon^\sigma_{33}(0,T)$ [63], d_{36} [63], c^E_{66} [66], $\varepsilon^{*\varepsilon}_{33}(\omega,T)$ [22]; for $K(H_{1-x}D_x)_2AsO_4$: $T_c(x)$ [52], $P_s(T)$ [52], $\Delta C_p(T)$ [52], $\varepsilon^\sigma_{33}(0,T)$ [51, 52], d_{36} [67], c^E_{66} [67], $\varepsilon^{*\varepsilon}_{33}(\omega,T)$ [22].

The fitting procedure will be explained on the example of the KH_2PO_4 crystal. With different chosen sets of the parameters ε_H and w_H, determining $\nu_c(0)$ from the condition of the free energy minimum, we find those values of ε_H, w_H, and $\nu_c(0)$ that reproduce properly the observed temperature curves of $P_s(T)$ and ΔC_p. The value of the effective dipole moment μ^-_{3H} in the ferroelectric phase is determined by fitting the theoretical temperature curves of spontaneous polarization and $\varepsilon''_{33}(\omega,T)$ as well as the value of saturation polarization to experiment. The value of μ^+_{3H} in the paraelectric phase is determined by fitting to experiment the theoretical temperature curve of longitudinal static dielectric permittivity, as well as the temperature and frequency dependences of $\varepsilon''_{33}(\omega,T)$.

In the ferroelectric phase the major task is to solve the system of equations for the order parameter $\eta^{(1)}(6)$ and ε_6. The temperature curves of spontaneous polarization and other characteristics are determined by those solutions of the system (2.9), (2.12) that satisfy the condition of the thermodynamic potential (2.10) minimum. It should be also beared in mind that the phase transition in the KH_2PO_4 crystal is of the first order. Therefore the parameter ν_c will be determined by minimization of the thermodynamic potential under condition that the calculated value of the first order phase transition temperature T_c corresponds to the experimental value. To determine the optimal values of ε_H, w_H, ν_c, μ_{3H} and deformational parameters ψ_{6H}, δ_{s6H}, δ_{a6H}, and δ_{16H} we explored the their influence on the temperature curves of $P_s(T)$, ΔC_p, ε_6, $\varepsilon^\varepsilon_{33}(0,T)$, $\varepsilon^\sigma_{33}(0,T)$ d_{36}, e_{36}, h_{36}, g_{36}, and c^E_{66}. As a result we obtained a set of the parameters ε_H, w_H, ν_{CH}, μ_{3H}, ψ_{6H}, δ_{s6H}, δ_{a6H}, and δ_{16H}, at which the calculated using the potential $g(6)$ temperature is $T_c = 122.5$ K, and the calculated temperature curves of $P_s(T)$, ΔC_p, ε_6, $\varepsilon^\varepsilon_{33}(0,T)$, $\varepsilon^\sigma_{33}(0,T)$, d_{36}, e_{36}, h_{36}, g_{36}, and c^E_{66} coincide with experimental data.

The value of the effective dipole moment μ^-_{3H} in the ferroelectric phase is determined by fitting the theoretical temperature curve of $\varepsilon''_{33}(\omega,T)$ as well as the value of saturation polarization to experiment (see [13]). Due to inconsistency of different experimental data for $\varepsilon^\sigma_{33}(0,T)$ in the paraelectric phase, we determine μ^+_{3H} by fitting to the experimental points for $\varepsilon''_{33}(\omega,T)$ [18]. In the same way we obtain the values of the model parameters for KD_2PO_4 and other crystals of the KH_2PO_4 type. Using (3.1) and the experimental data for T_c, $P_s(T)$, $\varepsilon^\sigma_{33}(0,T)$, and $\varepsilon''_{33}(\omega,T)$, by the described above method we determine the values of the parameters ν_c, μ^-_{3H}, μ^+_{3H} for partially deuterated crystals $K(H_{1-x}D_x)_2PO_4$.

The obtained optimal values of the theory parameters are presented in Table 2 for $K(H_{1-x}D_x)_2PO_4$ crystals, in Table 3 for $Rb(H_{1-x}D_x)_2PO_4$, and in Table 4 for $K(H_{1-x}D_x)_2AsO_4$. As one can see, to describe the observed temperature curves of polarization and static dielectric permittivity in the paraelectric phase, we should accept different values of the effective dipole moment μ_3 in ferroelectric and paraelectric phases, and $\mu_3^+ > \mu_3^-$. The dipole moment μ_3 is chosen in such a way in other papers too, including [36]. In [50] the difference of the ratio μ_3^+/μ_3^- from unity is explained by the existence of an underdampled soft mode in the crystal. Impossibility to describe both polarization and paraelectric static permittivity within the order-disorder model without introduction of two values of μ_3 for two phases indicates the applicability limits of the given model. Therefore, the proton ordering model should be extended by considering phonon degrees of freedom and anharmonisms.

x	T_c (K)	T_0 (K)	$\frac{\varepsilon}{k_B}$ (K)	$\frac{w}{k_B}$ (K)	$\frac{\nu_c}{k_B}$ (K)	$\mu_{3-}, 10^{-18}$ (esu · cm)	$\mu_{3+}, 10^{-18}$ (esu · cm)	χ_{33}^0
0.00	122.5	122.5	56.00	422.0	17.91	1.46	1.71	0.73
0.81	205.6	204.8	85.82	781.5	33.44	1.76	2.02	0.42
0.84	208.0	207.0	87.12	797.1	34.63	1.77	2.03	0.41
0.88	211.0	210.0	88.60	815.0	34.90	1.79	2.05	0.39
1.00	220.1	219.0	93.05	868.6	35.76	1.84	2.10	0.34

x	$\frac{\psi_6}{k_B}$ (K)	$\frac{\delta_{s6}}{k_B}$ (K)	$\frac{\delta_{a6}}{k_B}$ (K)	$\frac{\delta_{16}}{k_B}$ (K)	$c_{66}^0 \cdot 10^{-10}$ (dyn/cm^2)	e_{36}^0 (esu/cm^2)
0.00	−150.00	82.00	−500.00	−400.00	7.10	1000.00
0.81	−200.00	52.73	−957.39	−400.00	6.45	1914.77
0.84	−140.45	51.45	−977.27	−400.00	6.43	1954.55
0.88	−140.00	50.00	−1000.00	−400.00	6.40	2000.00
1.00	−138.64	45.64	−1068.18	−400.00	6.30	2136.36

Table 2. Optimal values of the model parameters for $K(H_{1-x}D_x)_2PO_4$ crystals.

x	T_c (K)	T_0 (K)	$\frac{\varepsilon}{k_B}$ (K)	$\frac{w}{k_B}$ (K)	$\frac{\nu_c}{k_B}$ (K)	$\mu_{3-}, 10^{-18}$ (esu · cm)	$\mu_{3+}, 10^{-18}$ (esu · cm)	χ_{33}^0
0.00	147.6	147.6	60.00	440.0	29.13	1.50	2.00	0.40
0.48	193.0	192.5	78.00	645.8	36.52	1.68	2.03	0.39
0.80	223.0	222.1	90.00	783.0	41.47	1.80	2.05	0.39

x	$\frac{\psi_6}{k_B}$ (K)	$\frac{\delta_{s6}}{k_B}$ (K)	$\frac{\delta_{a6}}{k_B}$ (K)	$\frac{\delta_{16}}{k_B}$ (K)	$c_{66}^0 \cdot 10^{-10}$ (dyn/cm^2)	e_{36}^0 (esu/cm^2)
0.00	−130.00	50.00	−500.00	−300.00	5.90	3000.00
0.48	−124.00	44.00	−620.00	−300.00	6.32	2400.00
0.80	−120.00	40.00	−700.00	−300.00	6.60	2000.00

Table 3. Optimal values of the model parameters for $Rb(H_{1-x}D_x)_2PO_4$ crystals.

x	T_c (K)	T_0 (K)	$\frac{\varepsilon}{k_B}$ (K)	$\frac{w}{k_B}$ (K)	$\frac{\nu_c}{k_B}$ (K)	$\mu_{3-}, 10^{-18}$ (esu · cm)	$\mu_{3+}, 10^{-18}$ (esu · cm)	χ^0_{33}
0.00	97.0	95.8	35.50	385.0	17.43	1.61	1.65	0.70
1.00	162.0	158.7	56.00	690.0	31.72	2.20	2.20	0.50

x	$\frac{\psi_6}{k_B}$ (K)	$\frac{\delta_{s6}}{k_B}$ (K)	$\frac{\delta_{a6}}{k_B}$ (K)	$\frac{\delta_{16}}{k_B}$ (K)	$c^0_{66} \cdot 10^{-10}$ (dyn/cm^2)	e^0_{36} (esu/cm^2)
0.00	−170.00	130.00	−500.00	−500.00	7.50	3000.00
1.00	−160.00	120.00	−800.00	−500.00	6.95	3000.00

Table 4. Optimal values of the model parameters for $K(H_{1-x}D_x)_2AsO_4$ crystals.

The calculated with these values differences between the Curie–Weiss temperatures of free and clamped crystals $T_0^\sigma - T_0^\varepsilon$ and the difference between the phase transition temperature and Curie-Weiss temperature $T_c - T_0^\sigma$ for $M(H_{1-x}D_x)_2XO_4$, along with data of other works are given in Table 5.

	$T_0^\sigma - T_0^\varepsilon$ (K)	$T_0^\sigma - T_0^\varepsilon$ (K)	$T_c - T_0^\sigma$ (K)	$T_c - T_0^\sigma$ (K)
KH_2PO_4	3.2	3.5 [60] 4.0 [68]	0.006	0.000 [35] 0.012 [69] 0.021 [70] 0.053 [51] 0.060 [71] 0.060 [11]
KD_2PO_4	3.9	6.7 [40]	1.135	0.73 [51] 1.5 [35] 1.5 [52] 2.3 [40]
RbH_2PO_4	2.3		0.024	0.000 [70] 0.060 [57] 0.076 [51]
KH_2AsO_4	5.5		1.182	0.716 [70] 1.55 [52] 1.82 [51]
KD_2AsO_4	5.8		3.338	3.63 [52]

Table 5. The differences $T_0^\sigma - T_0^\varepsilon$ and $T_c - T_0^\sigma$ for $M(H_{1-x}D_x)_2XO_4$ crystals.

The long-range interaction parameter ν_c could be also determined from the equation for the Curie-Weiss temperature T_0^ε, at which the susceptibility of a clamped crystal (3.12) has a peculiarity and $T_0^\sigma - T_0^\varepsilon = 3.5$ K. Then $\tilde{\nu}_c = 17.75$ K. However, at this value of $\tilde{\nu}_c$ we failed to find such a set of the values of the deformational parameters that would yield $T_c = 122.5$ and an agreement with experiment for the temperature dependences of piezoelectric coefficients. The observed differences $T_0^\sigma - T_0^\varepsilon$ and $T_c - T_0^\sigma$ were better described only with taking into account the tunneling in [11].

Let us evaluate now the physical characteristics of the $M(H_{1-x}D_x)_2XO_4$ crystals with the determined values of the model parameters and compare the obtained results with experimental data.

The calculated temperature curves of spontaneous polarization $P_s(T)$ for $K(H_{1-x}D_x)_2PO_4$ at different deuterations x along with experimental points are given in Fig. 4. In KH_2PO_4 a first order phase transition is observed, however, close to the second order. At deuteration the "first-orderness" of the phase transition increases.

The theoretical dependences $P_s(T)$ well describe the experimental temperature curve [35] for $x = 1.0$ and 0.80. At $x = 0.33$ and $x = 0.0$ starting from $\Delta T \sim 15$ K the calculated values of $P_s(T)$ are by ∼10% higher than the values of [35]. However, the proposed theory well describes the experimental [69, 72] $P_s(T)$ of KH_2PO_4. The calculated in [11] with taking into account tunneling values of $P_s(T)$ for KH_2PO_4 well agree with the results of [35]. The theory yields $P_{CH}/P_{SH} = 0.23$, whereas the values of this ratio obtained from experimental data are 0.36 [51, 52] and 0.14 [71]. For a deuterated crystal $P_{CD}/P_{SD} = 0.75$, which almost agrees with experimental 0.65 [35] and 0.724 [52].

In Fig. 5 we plot the calculated $P_s(T)$ along with the experimental data for KH_2PO_4, KD_2PO_4, RbH_2PO_4, KH_2AsO_4, and KD_2AsO_4.

The proposed theory provides a good quantitative description of the temperature dependence of polarization for these crystals. For RbH_2PO_4 we get $P_{CH}/P_{SH} = 0.33$, whereas the experiment yields 0.35 [51] or 0.30 [52]. For KH_2AsO_4 we get $P_{CH}/P_{SH} = 0,84$, whereas the experimental values are 0.86 [51] and 0.84 [52]. For KD_2AsO_4 the calculated ratio is $P_{CH}/P_{SH} = 0,91$ and the obtained in [52] value is 0.92. At the replacement K → Rb the spontaneous polarization decreases at all temperatures by about 10%, and the phase transition is still of the first order. At the replacement P→ As the saturation polarization increases from $5.0{\cdot}10^{-2}$ C/m^2 to $5.2{\cdot}10^{-2}$ C/m^2, with a very weak temperature dependence of $P_s(T)$ and a clear first order phase transition at $T = T_c$. At deuteration the saturation polarization increses up to $7.1{\cdot}10^{-2}$ C/m^2.

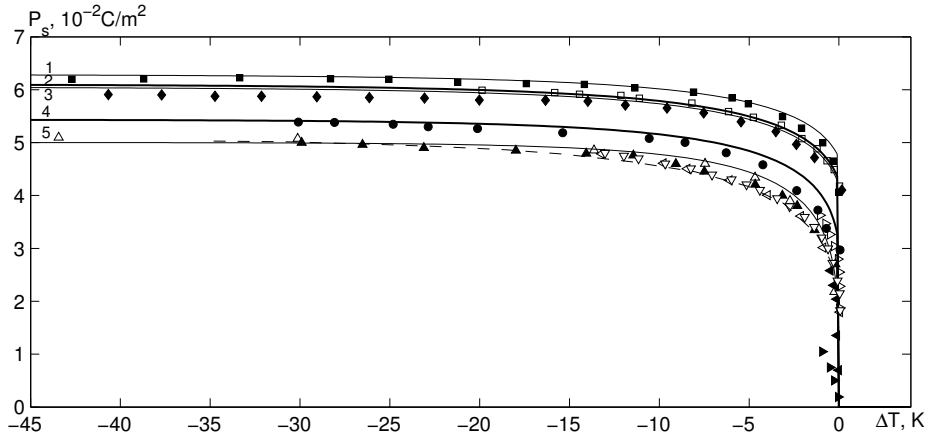

Fig. 4. Temperature dependence of spontaneous polarization of $K(H_{1-x}D_x)_2PO_4$ at different x: 1.0 — 1, ■ [35]; 0.84 — 2, ▫ [51]; 0.8 — 3, ♦ [35]; 0.33 — 4, ● [35]; 0.0 — 5, △ [54], ▲ [35], ◁ [72], ◀ [71], ▷ [69], ▶ [44], ▽ [51]. Symbols are experimental points; solid lines are present theoretical results; dashed line is the theoretical results of [11] for KH_2PO_4.

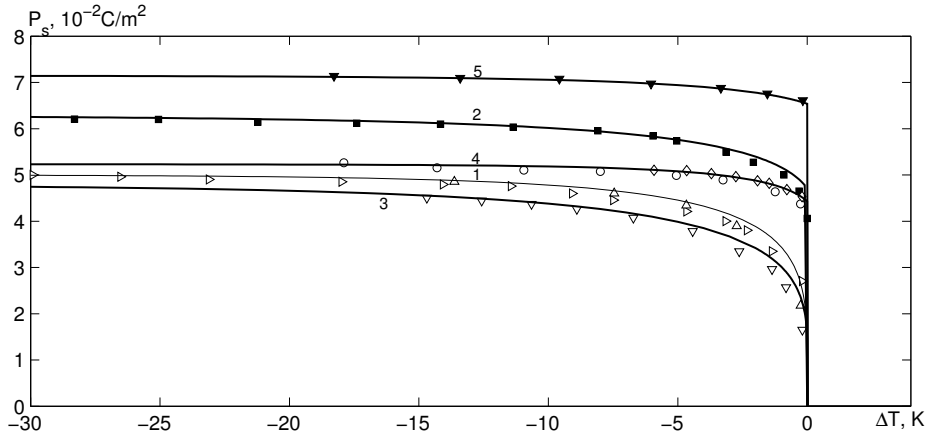

Fig. 5. Temperature dependence of spontaneous polarization of: KH_2PO_4 — 1, △ [54], ▷ [35]; KD_2PO_4 — 2, ■ [35]; RbH_2PO_4 — 3, ▽ [37]; KH_2AsO_4 — 4, ○ [52], ◇ [51]; KD_2AsO_4 — 5, ▼ [52]. Symbols are experimental points; solid lines are present theoretical results.

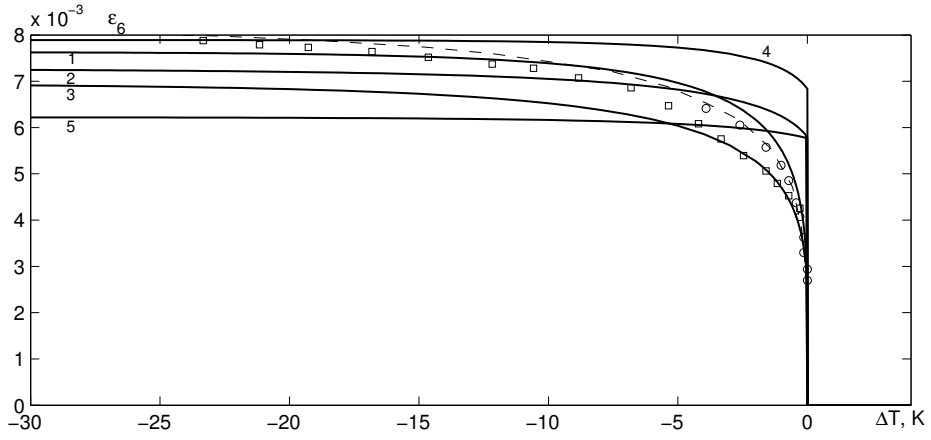

Fig. 6. Temperature dependence of spontaneous strain ε_6 for: KH_2PO_4 — 1, ▫ , [56], ○ , [55], KD_2PO_4 — 2, RbH_2PO_4 — 3, KH_2AsO_4 — 4, KD_2AsO_4 — 5. Symbols are experimental points; solid lines are present theoretical results; dashed line is the theoretical results of [11] for KH_2PO_4.

In Figure 6 we show the calculated temperature dependence of spontaneous strain ε_6 of KH_2PO_4, KD_2PO_4, RbH_2PO_4, KH_2AsO_4, KD_2AsO_4 crystals along with the experimental data for $\varepsilon_6(T)$ given in [55,56] for KH_2PO_4. As one can see, the calculated curve $\varepsilon_6(T)$ well agrees with experimental points, especially obtained in [56]. The temperature curve of ε_6 is qualitatively the same as of $P_s(T)$.

As seen in Figs. 7, 8, the proposed theory quantitatively well describes the temperature dependences of molar specific heat at constant pressure ΔC_p of the $K(H_{1-x}D_x)_2PO_4$, $Rb(H_{1-x}D_x)_2PO_4$, KH_2AsO_4, and KD_2AsO_4 crystals.

The experimental values of ΔC_p are determined by subtracting a lattice contribution to the specific heat, approximated by linear dependence in the phase transition region, from the total measured specific heat of the crystal. The analysis of the temperature dependences of polarization and proton molar specific heat on the theory parameters ε and w shows that the changes in ε at constant w hardly affects the values of P_s or ΔC_p, whereas at constant ε an increase in w moves the theoretical curve ΔC_p closer to the experimental points and increases convexity of the $P_s(T)$ curve. Therefore we choose such values of the parameters ε and w that properly describe both characteristics.

Let us consider now the longitudinal static dielectric permittivities of mechanically free and clamped crystals $M(H_{1-x}D_x)_2XO_4$. Above the transition temperature T_c at $\Delta T = T - T_c < 50°$ the Curie–Weiss law is obeyed [68] for the temperature curve of free dielectric permittivity: $\varepsilon_{33}^{\sigma}(0) \approx \frac{C_{\rm CW}}{T-T_0}$ ($C_{\rm CW}$ is the Curie–Weiss constant; T_0 is the Curie–Weiss temperature).

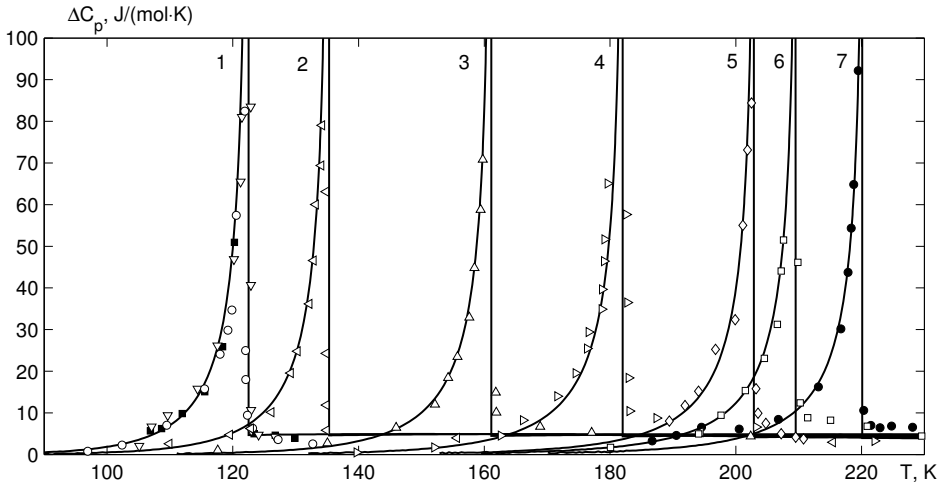

Fig. 7. Temperature dependences of specific heat of $K(H_{1-x}D_x)_2PO_4$ at different x: 0.0 — 1, ○ [46], ▼ [58], ■ [73]; 0.11 — 2, ◁ [46]; 0.34 — 3, △ [46]; 0.54 — 4, ▷ [46]; 0.78 — 5, ◇ [58]; 0.86 — 6, □ [46]; 1.0 — 7, ● [59]. Symbols are experimental data; solid lines are theoretical values obtained in the present work.

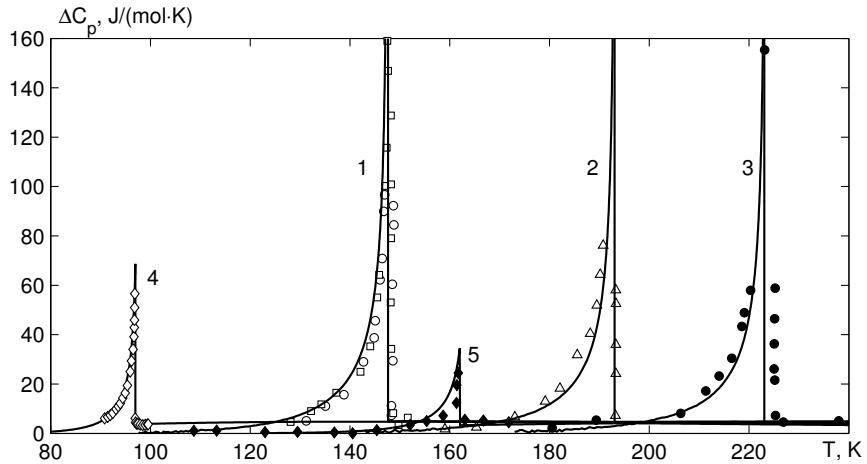

Fig. 8. Temperature dependences of specific heat of $Rb(H_{1-x}D_x)_2PO_4$ at different x: 0.0 — 1, ○ [57], □ [74]; 0.5 — 2, △ [57]; 0.8 — 3, ● [57]; KH_2AsO_4 — ◇ $\geq KD_2AsO_4$ — ♦ . Symbols are experimental data; solid lines are theoretical values obtained in the present work.

When the dielectric permittivity is measured at frequencies above the piezoelectric resonance frequency, the permittivity of a clamped crystal $\varepsilon_{33}^{\sigma}(0,T)$ is obtained. It also described by the Curie–Weiss law, with the same (within measurement error) value of $C_{\rm CW}$ as for the free crystal. It shows that the difference between the inverse permittivities of clamped and free crystals is temperature independent [75].

The calculated temperature dependences of inverse static dielectric permittivities of free $\varepsilon_{33}^{\sigma}(0,T)$ and clamped $\varepsilon_{33}^{\varepsilon}(0,T)$ $K(H_{1-x}D_x)_2PO_4$ crystals at different values of x, as well for RbH_2PO_4, KH_2AsO_4, and KD_2AsO_4 crystals along with experimental points are presented in Fig. 9. A perceptible dispersion of experimental data is seen for KH_2PO_4. We can well describe the temperature curves of $\varepsilon_{33}^{-1}(0,T)$, obtained in some papers, whereas the description of other experiments is worse, especially at $\Delta T > 50$ K. At large x the Curie–Weiss law for $(\varepsilon_{33}^{\sigma}(0,T))^{-1}$ and $(\varepsilon_{33}^{\varepsilon}(0,T))^{-1}$ is obeyed in a rather wide temperature range. With decreasing x this range narrows, and a notable non-linearity in the temperature dependence of $(\varepsilon_{33}^{\varepsilon,\sigma}(0,T))^{-1}$ appears. With increasing x the magnitudes of $\varepsilon_{33}^{\sigma}(0,T)$ and $\varepsilon_{33}^{\varepsilon}(0,T)$ increase in the paraelectric phase and decrease in the ferroelectric phase. The value of the longitudinal static permittivity increases at all temperatures at the isomorphic replacement K → Rb and decreases at P → As.

The calculated Curie-Weiss constants for $(\varepsilon_{33}^{\sigma}(0,T))^{-1}$ are shown in Table 6.

It is also shown that the inverse dielectric permittivity $(\varepsilon_{33}(0,T))^{-1}$ of the KH_2PO_4 crystal calculated without taking into account the piezoelectric coupling coincides with the values of $(\varepsilon_{33}^{\sigma}(0,T))^{-1}$ at $\Delta T < 50$ K, whereas at larger ΔT the curve $(\varepsilon_{33}(0,T))^{-1}$ goes above the $(\varepsilon_{33}^{\sigma}(0,T))^{-1}$ curve.

In Figure 10 we present the calculated temperature dependences of the coefficients of piezoelectric strain d_{36} and piezoelectric stress e_{36} for KH_2PO_4, $K(H_{0,12}D_{0,88})_2PO_4$, RbH_2PO_4, and KH_2AsO_4 crystals along with the experimental points.

A good quantitative description of the experimental data for d_{36} and the recalculated data for e_{36} is obtained. At $T \to T_c$ the coefficients d_{36} and e_{36} increase. In the ferroelectric phase the theoretical values of d_{36} and e_{36} rapidly decrease; this decrease is much faster than in the paraelectric phase. At deuteration the maximal values of d_{36} and e_{36} decrease. At extrapolation to zero stresses, the temperature dependence of d_{36} can be approximated by the Curie–Weiss law

$$d_{36} = d_{36}^{0} + \frac{B}{T - T_0}. \tag{3.1}$$

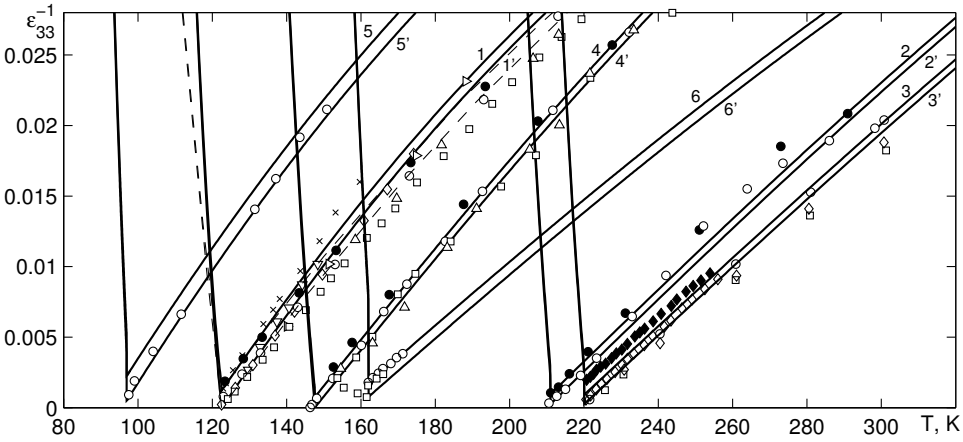

Fig. 9. Temperature dependences of inverse longitudinal permittivities of clamped $(\varepsilon_{33}^{\varepsilon})^{-1}$ (1) and free $(\varepsilon_{33}^{\sigma})^{-1}$ (2) crystals $K(H_{1-x}D_x)_2PO_4$: $x = 0.0$ — 1, 1′, ○ , ● [60], ▫ [78], ◇ [35], ▷ [76], ◁ [51], ▽ [79], △ [47], × [56]; $x = 0.88$ — 2, 2′, ○ [63], ● $((\varepsilon_{33}^{\sigma}-1)/4\pi$ [80] $- d_{36}^2$ [80]$/s_{66}^{E})4\pi+1$; $x = 1.0$ — 3, 3′, ♦ , ◇ [40], ○ [35], ▫ [38]; RbH_2PO_4 — 4, 4′ ○ [63], ● $((\varepsilon_{33}^{\sigma}$-1)$/4\pi$ [80] $- d_{36}^2$ [80]$/s_{66}^{E})4\pi+1$, ▫ [82], △ [76]; KH_2AsO_4 — 5, 5′ ○ [51]; KD_2AsO_4 — 6, 6′ ○ [52], ▫ [81]. Symbols are experimental data; solid lines are theoretical values obtained in the present work; dashed lines are theoretical results of [11] for KH_2PO_4.

	$K(H_{1-x}D_x)_2PO_4$						RbH_2PO_4	$K(H_{1-x}D_x)_2AsO_4$	
x	0.00	0.33	0.55	0.80	0.88	1.00		0.00	1.00
$C_{\rm CW}$(K)	2614	3033	3342	3744	3886	4104	3042	2402	4328

Table 6. The calculated Curie–Weiss constants for $M(H_{1-x}D_x)_2XO_4$.

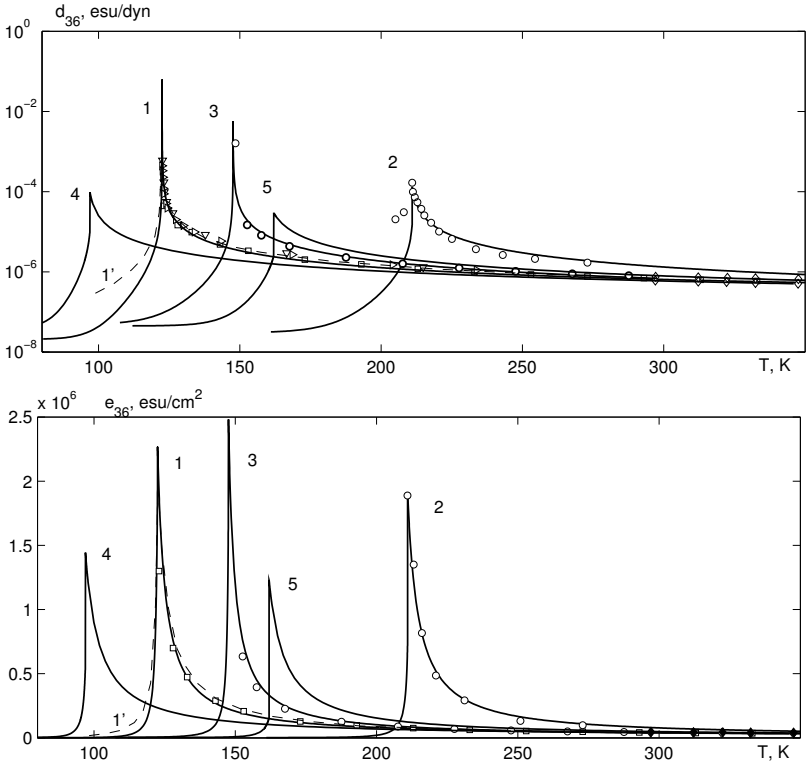

Fig. 10. Temperature dependences of the coefficient of piezoelectric strain d_{36} of KH_2PO_4 — 1, ▫ [60], ▽ [61], ▷ [62]; $K(H_{0.12}D_{0.88})_2PO_4$ — 2, ○ [63]; RbH_2PO_4 — 3, ○ [63]; KH_2AsO_4 — 4, ◇ [67]; KD_2AsO_4 — 5, ♦ [67] and of the coefficient piezoelectric stress e_{36} of KH_2PO_4 — 1, ▫ [60]; $K(H_{0.12}D_{0.88})_2PO_4$ — 2, ○ $-d_{36}$ [63]/s^E_{66} [66]; RbH_2PO_4 — 3, ○ $-d_{36}$ [63]/s^E_{66} [66]; KH_2AsO_4 — 4, ◇ $-d_{36}/s^E_{66}$ [67]; KD_2AsO_4 — 5, ♦ $-d_{36}/s^E_{66}$ [67]. Symbols are experimental data; solid lines are theoretical values obtained in the present work; dashed lines are theoretical results of [11] for KH_2PO_4.

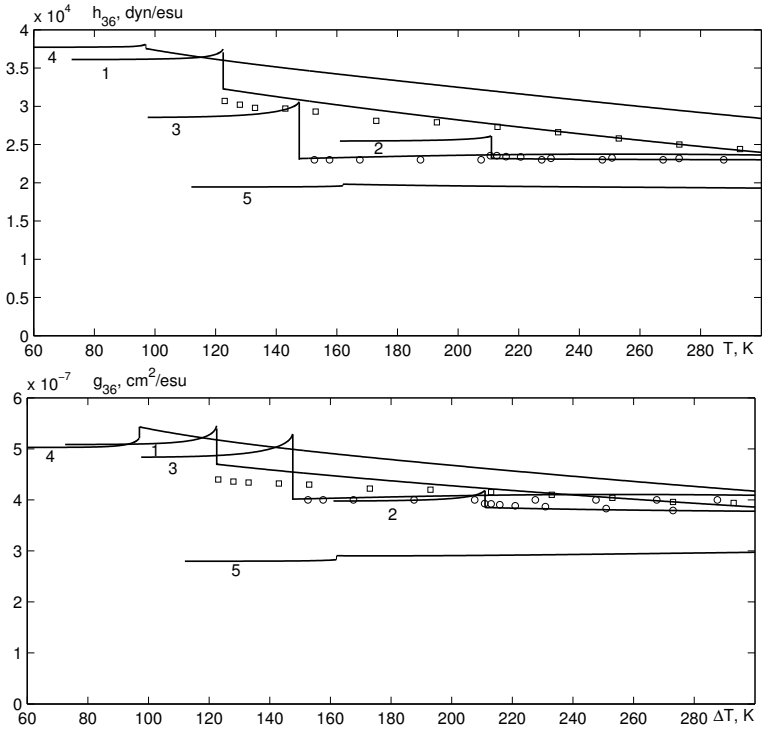

Fig. 11. Temperature dependences of the constant piezoelectric stress h_{36} of KH_2PO_4 — 1, ▫ [60]; $K(H_{0.12}D_{0.88})_2PO_4$ — 2, ○ $-d_{36}/(s^E_{66}\chi^\sigma_{33} - d^2_{36})$ [63]; RbH_2PO_4 — 3, ○ [63]; KH_2AsO_4 — 4; KD_2AsO_4 — 5 and of the constant of piezoelectric strain g_{36} of KH_2PO_4 — 1, ▫ [60]; $K(H_{0.12}D_{0.88})_2PO_4$ — 2, ○ $-d_{36}/\chi^\sigma_{33}$ [63]; RbH_2PO_4 — 3, ○ – [63]; KH_2AsO_4 — 4; KD_2AsO_4 — 5.

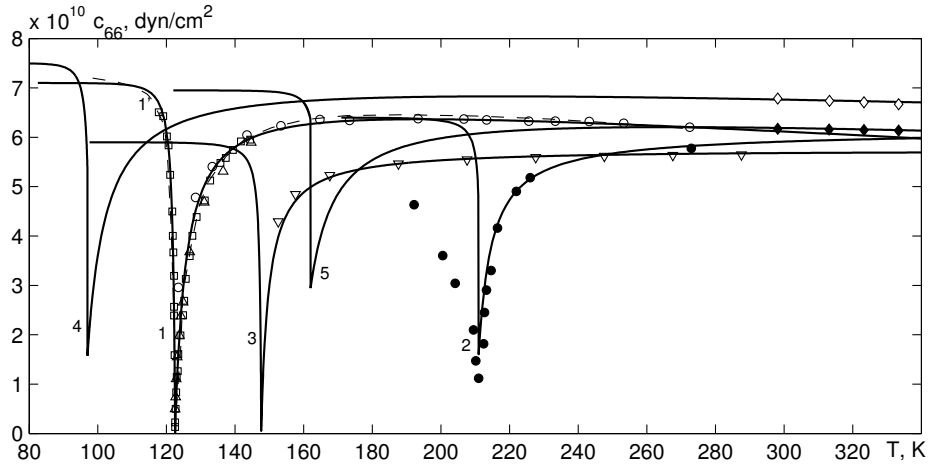

Fig. 12. Temperature dependence of elastic constants c_{66}^E of KH_2PO_4 — 1, ○ [60], ▫ [65], △ [64]; $K(H_{0.12}D_{0.88})_2PO_4$ — 2, ○ $-1/s_{66}^E$ [66]; RbH_2PO_4 — 3, ○ $-1/s_{66}^E$ [66]; KH_2AsO_4 — 4, ◇ $-1/s_{66}^E$ [67]; KD_2AsO_4 — 5, ◇ $-1/s_{66}^E$ [67]. Solid lines are theoretical values obtained in the present work; dashed lines are theoretical results of [11] for KH_2PO_4.

The values of d_{36}^0 and B for KH_2PO_4 estimated in [83] are $B = 1.26 \cdot 10^{-4}$ esu/dyn, $d_{36}^0 \cong -8 \cdot 10^{-8}$ esu/cm^2. Of course, near the Curie point the temperature independent term can be neglected.

The temperature dependences of the constants of piezoelectric stress h_{36}^T and piezoelectric strain g_{36}^T of MH_2XO_4 and $K(H_{0,12}D_{0,88})_2PO_4$, along with the data of [60] and recalculated values of h_{36}^T and g_{36}^T are shown in Fig. 11.

In the paraelectric phase the values of the constants were recalculated using the relations

$$h_{36}^T = \frac{e_{36}^T}{\chi_{33}^{T\varepsilon}}, \quad g_{36}^T = \frac{d_{36}^T}{\chi_{33}^{T\sigma}}. \tag{3.2}$$

The calculated temperature dependences of h_{36}^T and g_{36}^T at $T > T_c$ well agree with the data of [60] and with the values recalculated using the experimental points of [63]. Since the dielectric susceptibility is described by the Curie–Weiss law

$$\chi_{33}^{T\sigma} \approx \frac{C_{\rm CW}}{4\pi(T - T_0)}, \tag{3.3}$$

where for KH_2PO_4 $C_{\rm CW} = 3250$ K [75]. Using (3.2), taking into account (3.1) and (3.3), we obtain

$$g_{36}^T \approx \frac{4\pi B}{C_{\rm CW}}. \tag{3.4}$$

With the estimated values of B [83] and $C_{\rm CW}$ we find $g_{36}^T = 4.87 \cdot 10^{-7}$ cm^2/esu.

In the ferroelectric phase for the mechanically free crystal ($\sigma_6 = 0$) the polarization P_s and strain ε_6 are related as follows

$$P_s = \frac{\chi_{33}^{T\varepsilon}}{d_{36}^T}\varepsilon_6 = \frac{\varepsilon_6}{g_{36}^T}. \tag{3.5}$$

Therefore, at $T < T_c$ the temperature dependence of the constants of piezoelectric strain and stress were calculated using the relations

$$g_{36}^T = \frac{\varepsilon_6}{P_s},$$

and

$$h_{36}^T = g_{36}^T c_{66}^{TP}.$$

For KH_2PO_4 at $T = 110$ K, as shown in [83], $\frac{\varepsilon_6}{P_s} = 1/1.85 \cdot 10^6$ од. CGSE $= 5.41 \cdot 10^{-7}$ cm^2/esu. Theoretical calculations yield $g_{36} = 5.2 \cdot 10^{-7}$ cm^2/esu.

As seen in Fig. 11, the constants h_{36}^T are g_{36}^T slightly decrease with increasing temperature and have jumps $T = T_c$. Since they have no peculiarities at the ferroelectric phase transition, they are called "true" piezoelectric constants of the crystals.

The temperature dependences of the calculated isothermic elastic constants c_{66}^{TE} and c_{66}^{TP} for KH_2PO_4, $K(H_{0,12}D_{0,88})_2PO_4$, RbH_2PO_4, KH_2AsO_4, and KD_2AsO_4 crystals well agree with experimental data (Fig. 12). At the transition temperature the elastic constant c_{66}^{TE} of KH_2PO_4 and RbH_2PO_4 tends to zero, whereas it has a minimum in other crystals. An increase in deuteration x increases the minimal values of c_{66}^{TE} at $T = T_c$. In the paraelectric phase c_{66}^{TE} increases with increasing the distance from the transition temperature ΔT; this increase is much slower than in the ferroelectric phase.

The analysis of experimental points for KH_2PO_4 shows that the Curie-Weiss law is obeyed also for the quantities

$$\frac{1}{c_{66}^{TE}} - \frac{1}{c_{66}^{TP}} = s_{66}^{TE} - s_{66}^{TP} = \frac{D}{T - T_0},$$

where $D = 4,6 \cdot 10^{-11}$ cm^2·K/dyn. In RbH_2PO_4 $D = 15.6 \cdot 10^{-11}$ cm^2·K/dyn [83].

The elastic constant c_{66}^{TP} at $T < T_c$ does not change with temperature, has a downward jump at $T = T_c$, and slightly linearly decreases with increasing temperature in the paraelectric phase.

IV. CONCLUDING REMARKS

In the present paper using the modified proton ordering model without tunneling, within the framework of the four-particle cluster approximation we develop a theory of thermodynamic and longitudinal dielectric, piezoelectric, and elastic properties of the KD_2PO_4 type ferroelectrics. A thorough numerical analysis of the variation of the calculated characteristics of the KD_2PO_4 and KH_2PO_4 type ferroelectrics with the values of the theory parameters and deformational potentials. Optimal sets of these parameters as well as "seed" characteristics for the studied crystals are determined; they provide a satisfactory description of available experimental data.

The physical characteristics of partially deuterated crystals of the $K(H_{1-x}D_x)_2PO_4$ type are calculated in the mean crystal approximation; a good quantitative description of available experimental data is obtained.

It is established that taking into account the piezoelectric coupling hardly affects spontaneous polarization of molar specific heat, but leads to the appearance of difference between the dielectric permittivities of mechanically clamped and free crystals. It is also shown that within the developed theory the piezoelectric coupling essentially affects the difference between the phase transition temperature and Curie–Weiss temperature of free crystals. However, a good agreement with experiment in the $K(H_{1-x}D_x)_2PO_4$ crystals can be obtained only with taking into account tunneling. At the same time, tunneling practically does not affect the piezoelctric and elastic characteristics of the studies crystals.

[1] R. R. Levitsky, I. R. Zachek, A. S. Vdovych, S. I. Sorokov, Condens. Matter Phys. **12**, 75 (2009).

[2] I. V. Stasyuk, I. N. Biletskii, *Preprint of the Bogolyubov Institute for Theoretical Physics*, in Russian (ITP-83-93R, Kyiv, 1983).

[3] I. V. Stasyuk, I. N. Biletskii, O. N. Styagar, Ukr. Phys. J. **31**, 567 (1986).

[4] I. V. Stasyuk, R. R. Levitskii, I. R. Zachek, A. P. Moina, Phys. Rev. B **62**, 6198 (2000).

[5] R. R. Levitskii, B. M. Lisnii, J. Phys. Stud. **7**, 431 (2003) [in Ukrainian].

[6] R. R. Levitskii, B. M. Lisnii, Phys. Status Solidi B **241**, 1350 (2004).

[7] I. V. Stasyuk, R. R. Levitskii, A. P. Moina, B. M. Lisnii, Ferroelectrics, **254**, 213 (2001).

[8] B. M. Lisnii, R. R. Levitskii, O. R. Baran, Phase Transitions, **80**, 25 (2007).

[9] I. V. Stasyuk, R. R. Levitskii, A. P. Moina, O. V. Velychko, Ukr. J. Phys. Reviews **4**, 3 (2008).

[10] I. V. Stasyuk, N. M. Kaminska, Ukr. Phys. J. **19**, 237 (1974) [in Ukrainian].

[11] R. R. Levitskii, B. M. Lisnii, J. Phys. Stud. **6**, 91 (2002) [in Ukrainian].

[12] I. V. Stasyuk, R. R. Levitskii, N. A. Korinevskii, Phys. Status Solidi B **91**, 541 (1979).

[13] R. R. Levitskii, I. R. Zachek, A. S. Vdovych, Preprint ICMP–06–08U, Lviv, 2006 [in Ukrainian].

[14] I. V. Stasyuk, R. R. Levitskii, Phys. Status Solidi B **39**, K35 (1970).

[15] R. R. Levitskii, N. A. Korinevskii, I. V. Stasyuk, Ukr. Phys. J. **19**, 1289 (1974) [in Russian].

[16] R. Blinc, S. Svetina, Phys. Rev. **147**, 423 (1966).

[17] R. R. Levitskii, A. P. Moina, B. M. Lisnii, Preprint ICMP–00–12U, Lviv (2000).

[18] A. A. Volkov, G. V. Kozlov, S. P. Lebedev, I. A. Velychko, Fiz. Tverd. Tela **21**, 3304 (1979) [in Russian].

[19] I. P. Kaminov, Phys. Rev. **138**, 1539 (1965).

[20] R. M. Hill, S. K. Ichiki, Phys. Rev. **132**, 1603 (1963).

[21] L. P. Pereverzeva, Yu. M. Poplavko, I. S. Rez, L. I. Kuznetsova, Kristallografiya **21**, 981 (1976) [in Russian].

[22] A. A. Volkov, G. V. Kozlov, S. P. Lebedev, A. M. Prokhorov, Ferroelectrics **25**, 531 (1980).

[23] R. R. Levitskii, I. V. Stasyuk, H. A. Korinevsky, Ferroelectrics **21**, 481 (1978).

[24] N. A. Korinevskii, R. R. Levitskii, Teor. Mat. Fiz. **42**, 416 (1980) [in Russian].

[25] K. E. Gauss, H. Happ, Phys. Status Solidi B **78**, 133 (1976).

[26] S. G. Zhukov, V. A. Kulbachinskii, P. S. Smirnov, B. A. Strukov, S. M. Chudinov, Izv. Akad. Nauk SSSR, Ser. Fiz. **49**, 255 (1985) [in Russian].

[27] A. Baddur, B. A. Strukov, I. A. Velichko, V. N. Setkina, Kristallografiya **17**, 1065 (1972) [in Russian].

[28] J. Skalyo, B. C. Jr. Frazer, G. Shirane, W. B. Daniels, J. Phys. Chem. Solids **30**, 2045 (1969).

[29] M. Kasahara, I. Tatsuzaki, J. Phys. Soc. Jpn **50**, 551 (1981).

[30] B. A. Strukov, M. Amin, A. S. Sonin, Fiz. Tverd. Tela **8**, 2421 (1967) [in Russian].

[31] E. N. Volkova, Yu. S. Podshivalov, L. N. Rashkovich, B. A. Strukov, Izv. Akad. Nauk SSSR, Ser. Fiz. **39**, 787 (1975) [in Russian].

[32] E. Litov, E. A. Uehling, Phys. Rev. B, **1**, 3713 (1970).

[33] V. A. Kramarenko, E. N. Volkova, M. D. Tsibizova, in *XI All-Union conference on physics of ferroelectrics. Book of Abstracts. Vol. 2* (Kiev, IF AN USSR, 1986) p. 28.

[34] E. N. Volkova, V. A. Kramarenko, M. D. Tsibizova, Pis'ma Zh. Tekh. Fiz. **14**, 408 (1988) [in Russian].

[35] G. A. Samara, Ferroelectrics **5**, 25 (1973).

[36] G. A. Samara, Phys. Lett. A **25**, 664 (1967).

[37] P. Gilletta, M. Chabin, Phys. Status Solidi B **100**, K77 (1980).

[38] B. Breziria, A. Fouskova, P. Smutny, Phys. Status Solidi A **11**, K149 (1972).

[39] T. R. Sliker, S. R. Burlage, J. Appl. Phys. **34**, 1837 (1963).

[40] R. M. Hill, S. K. Ichiki, Phys. Rev. **130**, 150 (1963).

[41] G. Luther, Ferroelectrics **12**, 243 (1976).

[42] V. V. Meriakri, E. F. Ushatkin, In *Fizicheskie metody issledovanija neorganicheskikh meterialov* [Physical methods of investigation of inorganic materials] (Nauka, Moskva, 1981).

[43] A. B. Sherman, D. Vayda, I. A. Velichko, O. S. Gut-

ner, V. V. Lemanov, Fiz. Tverd. Tela **13**, 3716 (1971) [in Russian].
[44] I. Hazario, J. A Gonzalo, Solid State Commun. **7**, 1305 (1969).
[45] G. M. Yoiacano, J. F. Balashio, W. Osborne, Appl. Phys. Lett. **24**, 455 (1974).
[46] B. A. Strukov, A. Baddur, V. A. Koptsik, I. A. Velychko, Fiz. Tverd. Tela **14**, 1034 (1972) [in Russian].
[47] E. N. Volkova, Candidate dissertation (Moskow, 1991) [in Russian].
[48] K. Deguchi, E. Nakamura, E. Okaue, N. Aramaki, J. Phys. Soc. Jpn, **51**, 3575 (1982).
[49] E. N. Volkova, B. M. Berezhnoy, A. N. Izrailenko, A. V. Mishchenko, L. N. Rashkovich, Izv. Akad. Nauk SSSR, Ser. Fiz. **35**, 1858 (1971) [in Russian].
[50] M. Tokunaga, J. Phys. Soc. Jpn. **56**, 1653 (1987).
[51] M. Chabin, P. Gilletta, Ferroelectrics, **15**, 149 (1977).
[52] C. W. Fairall, W. Reese, Phys. Rev. B, **6**, 193 (1972).
[53] G. V. Kozlov, S. P. Lebedev, A. M. Prokhorov, A. A. Volkov, J. Phys. Soc. Jpn, **49**, 188 (1980).
[54] G. G. Wiseman, IEEE Trans. Electron Devices **16**, 588 (1969).
[55] P. Bastie, J. Bornarel, J. Lajzerowicz, M. Vallade, J. R. Schneider, Phys. Rev. B **12**, 5112 (1975).
[56] J. Kobayashi, Y. Uesu, I. Mizutani, Y. Enomoto, Phys. Status Solidi A **3**, 63 (1970).
[57] B. A. Strukov, A. Baddur, V. N. Zinenko, A. V. Mishchenko, V. A. Kopsik, Fiz. Tverd. Tela **15**, 1388 (1973) [in Russian].
[58] B. A. Strukov, M. Amin, V. A. Kopsik, J. Phys. Soc. Jpn **28**, 207 (1970).
[59] W. Reese, L. P. May, Phys. Rev. **167**, 504 (1968).
[60] W. Mason, *Piezoelectric Constants and Their Application to Ultrasonics* (Van Nostrand, New York, 1950).
[61] W. Bantle, C. Caflish, Helv. Phys. Acta **16**, 235 (1943).
[62] A. Von Arx, W. Bantle, Helv. Phys. Acta **16**, 211 (1943).
[63] L. A. Shuvalov, I. S. Zheludev, A. V. Mnatsakanyan, Ts. Zh. Ludupov, I. Fiala, Izv. Akad. Nauk SSSR, Ser. Fiz. **31**, 1919 (1967) [in Russian].
[64] C. W. Garland, D. B. Novotny, Phys. Rev. **177**, 971 (1969).
[65] E. M. Brody, H. Z. Cummins, Phys. Rev. Lett. **21**, 1263 (1968).
[66] L. A. Shuvalov, A. V. Mnatsakanyan, Sov. Phys. Crystallogr. **11**, 210 (1966).
[67] R. S. Adhav, J. Appl. Phys. **39**, 4095 (1968).
[68] H. Baumgartner, Helv. Phys. Acta **24**, 326 (1951).
[69] J. W. Benepe, W. Reese, Phys. Rev. B **3**, 3032 (1971).
[70] V. G. Vaks, N. E. Zein, B. A. Strukov, Phys. Status Solidi A **30**, 801 (1975).
[71] B. A. Strukov, M. A. Korzhuev, A. Baddur, V. A. Kopsik, Fiz. Tverd. Tela **13**, 1872 (1971) [in Russian].
[72] G. A. Samara, Ferroelectrics, **22**, 925 (1979).
[73] W. Reese, L. F. May, Phys. Rev. **162**, 510 (1967).
[74] M. Amin, B. A. Strukov, Fiz. Tverd. Tela, **10**, 3158 (1968) [in Russian].
[75] F. Jona, G. Shirane, *Ferroelectric Crystals* (Pergamon Press, Oxford, 1962).
[76] A. S. Vasilevskaya, A. S. Sonin, Fiz. Tverd. Tela, **13**, 1550 (1971) [in Russian].
[77] R. R. Levitskii, B. M. Lisnii, O. R. Baran, Condens. Matter Phys. **4**, 523 (2001).
[78] K. Deguchi, E. Nakamura, J. Phys. Soc. Jpn, **49**, 1887 (1980).
[79] R. J. Mayer, J. L. Bjorkstam, J. Phys. Chem. Solids **23**, 619 (1962).
[80] B. A. Strukov, A. Baddur, I. A. Velychko, Fiz. Tverd. Tela **13**, 2484 (1971) [in Russian].
[81] R. Blinc, M. Burgar, A. Levstik, Solid State Commun. **12**, 573 (1973).
[82] L. P. Pereverzeva, Izv. AN SSSR, ser. fiz. **31**, 1919 (1967) [in Russian].
[83] W. Kanzig, *Ferroelectrics and Antiferroelectrics* (Academic Press, New York, 1957).

ПОЗДОВЖНІ ДІЕЛЕКТРИЧНІ, П'ЄЗОЕЛЕКТРИЧНІ, ПРУЖНІ ТА ТЕПЛОВІ ВЛАСТИВОСТІ СЕГНЕТОЕЛЕКТРИКІВ ТИПУ KH_2PO_4

Р. Р. Левицький[1], І. Р. Зачек[2], А. С. Вдович[1], А. П. Моїна[1]
[1]*Інститут фізики конденсованих систем НАН України вул. Свєнціцького, 1, Львів, 79011, Україна*
[2]*Національний університет "Львівська політехніка" вул. С. Бандери, 12, 79013, Львів, Україна*

У межах модифікованої моделі протонного впорядкування сегнетоелектриків типу KH_2PO_4 з урахуванням лінійного за деформацією ε_6 внеску в енергію протонної системи, але без урахування тунелювання в наближенні чотиричастинкового кластера отримано відповідні термодинамічні потенціали. Використовуючи відповідні рівняння стану, розраховано спонтанну поляризацію, поздовжню діелектричну проникність механічно затиснутого й механічно вільного кристалів, їхні п'єзоелектричні характеристики, пружні сталі та молярну теплоємність. При належному виборі мікропараметрів отримано добрий кількісний опис наявних експериментальних даних для сегнетоелектриків типу $K(H_{1-x}D_x)_2PO_4$.